CDF/ANAL/BOTTOM/CDFR/6978
Revision 0.1
May 18, 2004

CDF Search for the $\Theta_c^0(3099)$ State Reported by the H1 Experiment

Y.S. Chung[a], E. Gerchstein[b], D. Litvintsev[c], M. Neubauer[d] ,
J. Russ[b] , M.-J. Wang[e] , F. Würthwein[d]
([a] *University of Rochester, Rochester, N.Y.*)
([b] *Carnegie Mellon University, Pittsburgh, PA*)
([c] *Fermi National Accelerator Laboratory, Batavia, IL*)
([d] *University of California at San Diego, San Diego, CA*)
([e] *Academia Sinica, Taipei, Taiwan*)

May 18, 2004

Abstract

The long-standing question of whether there are 5-quark baryons has been reinvigorated in the past year by multiple reports of the existence of a baryon decaying to a KN final state with positive strangeness. This state, the $\Theta(1540)$, is manifestly exotic and had been predicted in 1997 as the lightest member of an anti-decuplet of states on the basis of a chiral soliton model by Diakonov, Petrov, and Polyakov [1]. There should be a charmed analog of this decuplet. Charmed pentaquarks had been predicted much earlier by other authors based on different models. The H1 experiment recently reported the observation of a narrow baryon at 3099 MeV/c^2 decaying to D*p + c.c. [3] This state is a candidate for the charmed pentaquark Θ_c or perhaps an excited state thereof. This note describes the search for this state in CDF data.

1 Introduction

Searches for 5-quark baryons, characterized by so-called exotic quantum numbers, i.e., quantum numbers that cannot be obtained from the minimal 3-quark baryon configurations, have taken place since the introduction of QCD and the quark model by Gell-Mann and Salam in 1963. Initially, much attention was focussed on baryons with positive strangeness, which required an $\bar{s}$ quark and hence did not fit into the standard 3-quark configuration. In the 1980s Lipkin and others noted that 5-quark configurations with a $\bar{c}$ quark might be bound in some models. Until 2002 all searches for such states were negative.

On the theory side a chiral soliton model was developed in 1997 by Diakonov, Petrov, and Polyakov [1] to explore the question of why so few of the allowed baryonic resonant states in 3-quark models were actually observed. One of the predictions of this model was the existence of an anti-decuplet of pentaquark states that should decay strongly, but with narrow widths because of internal chiral constraints on the wavefunctions. The lightest state, termed the Θ, was predicted to have a mass around 1540MeV/c^2 , with a width of 15MeV/c^2 . Nothing much happened with this picture until the Spring8 experiment reported marginal evidence for a narrow K^+ n state at 1540 MeV/c^2 in low energy photoproduction. The CLAS spectrometer at JLAB provided supporting evidence of this state in photodisintegration of the deuteron, again at low energy. A variety of other observations have been reported, all with somewhat marginal statistics and significantly different masses and widths. A CDF search for the Θ will be reported separately.

In March the H1 experiment at HERA reported a striking signal for a charmed pentaquark, terms the Θ_c. Jaffe and Wilczek adapted the chiral soliton model to include charm and had predicted a Θ_c mass near 2710 MeV/c^2 , below threshold for the strong decay into DN. [2] The H1 state is considerably more massive than this and decays strongly into D^*p or its charge conjugate state. It is suggested that this may be an excited state of the Θ_c. The width of this state is consistent with experimental resolution, less than 15 MeV/c^2 . It is of great interest to see if CDF can confirm the existence of this state.

We should note that the production mechanism at CDF for both the strange and charmed pentaquarks is very different from the low energy processes that have produced the only evidence thus far. For the $\Theta(1540)$, the Spring8 and CLAS experiments found that the ratio of pentaquark production to $\Lambda(1520)$ production was large, of order 1/4 to 1/3. No high energy hadroproduction experiment has reported positive evidence for this state. CDF has already reported that we do not confirm another reported member of the anti-decuplet, the $\Xi^{--}(1862)$ reported by the CERN NA49 experiment (150 GeV pp). A negative result of our CDF search does not imply that the H1 observation is incorrect. It states that *if* the H1 report is correct, then pentaquark production in low-pt DIS is much more significant that it is in high-energy $\bar{p}p$ collisions at similar η, p_T values.

2 Search Strategy

The following 4-track decay chains were studied in this analysis:

$$\begin{array}{llll} \overline{\Theta_c} \to & \mathrm{D}^{*+}\bar{\mathrm{p}}_{dec}(\mathrm{p}_{\mathrm{dec}}) & D^{**} \to & \mathrm{D}^{*+}\pi_{dec} \\ & \hookrightarrow \quad \mathrm{D}^0\pi^+_{slow} & & \hookrightarrow \quad \mathrm{D}^0\pi^+_{slow} \\ & \qquad \hookrightarrow \mathrm{K}^-\pi^+_{\mathrm{D}^0} & & \qquad \hookrightarrow \mathrm{K}^-\pi^+_{\mathrm{D}^0} \end{array} \tag{1}$$

where Θ_c denotes a pentaquark state and D^{**} jointly denotes p-wave orbital excitations $\mathrm{D}_1(2420)^0$ and $\mathrm{D}_2^*(2460)^0$. The decays $\mathrm{D}^{**} \to \mathrm{D}^{*+}\pi$ were used as reference channels.

As the pentaquark state decay chain contains proton the PID will have to be applied to extract proton tracks. The important first step in the study is to validate a procedure for identifying protons in the momentum range of interest.

3 Simulation

In order to establish the proton momentum range, we have used realistic Monte Carlo, following the B Monte Carlo group's procedures, for pentaquark studies. The assumptions in the generator and decay steps are

1. the pentaquark $\mathrm{p_T}$ spectrum is similar to the measured CDF prompt J/ψ spectrum (corrected) [4], since both states have similar mass.

2. the η dependence is flat for $|\ \eta\ | < 1.5$.

3. the pentaquark decay spectrum is isotropic. We ignore spin correlations between the proton and the D^*.

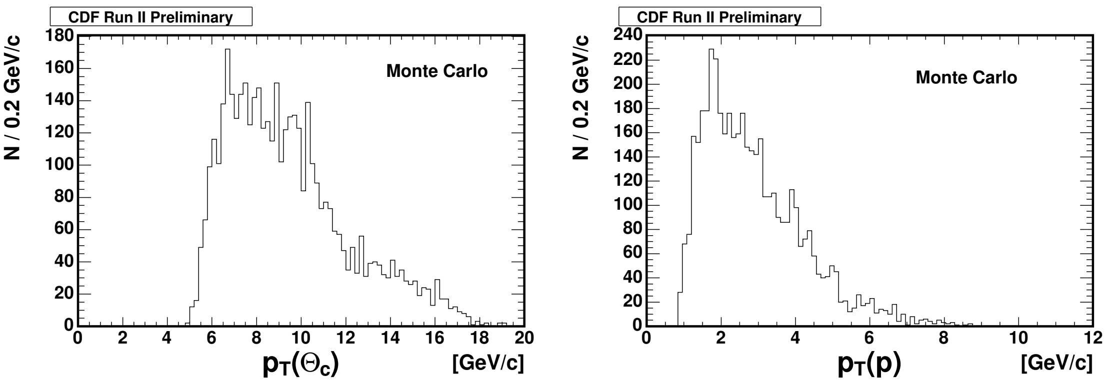

Figure 1: p_T spectra of Θ_c and its decay proton produced after analysis cuts. `FAKE_EVENT` with input $\mathrm{J}\psi$ p_T spectrum followed by realistic simulation chain were used to generate Θ_c spectrum

Assumption (1) is based on the general observation that the mean $\mathrm{p_T}$ for hadroproduction depends chiefly on the hadron mass and very little on internal quantum numbers.

Assumption (2) is standard for particles whose mass is small compared to the Tevatron collider energy (2 TeV). Assumption (3) follows from our understanding of the insensitivity of detection efficiency to spin correlations, e.g., in J/ψ studies. Polarization effects in that case are 10% effects, which are unimportant in fixing the proton p_T scale or the search sensitivity.

The predicted mass difference resolution for pentaquark signal at the mass reported by H1 Collaboration is 2.5 MeV/c^2.

4 Offline tracks

Offline tracks were treated according to the recommendations given by the B group for offline software version 5.3.1 as follows:

- ProcessName is set to `PROD_PHYSICS_CDF` and PassName 11A as input parameters to the *CalibrationManager* . Pass 13 sets up the correct alignment tables for the different run ranges.
- Additional layers of material were added to the silicon geometry according to the note[6]
- L00 alignment was turned off in the *SiliconGeometryMenu*
- Default tracks were required to have at least 16 COT stereo hits and 20 COT axial hits, and more then 2 axial silicon hits.
- Slow pion track candidates were required to have at least 4 silicon axial hits and no COT hits or at least 3 silicon axial hits and 10 COT axial and 10 COT stereo hits
- To correct for the energy losses and multiple scattering in the silicon detector tracks were refit using Kalman refitter taking into account appropriate masses for different candidates (K,π and p) participating in decay chains under study
- L00 hits were dropped
- COT covariance matrix was rescaled with scaling factors 21.72, 11.57, 14.64, 1.71, 1.544 for curvature, d_0, ϕ_0, z_0, and λ, accordingly.
- COT track curvature was rescaled using the *corrCOT()* method of *TrackRefitter* to correct for energy loss in the COT volume.

5 Data Sample

The analysis is based on data comprising an integrated $\mathcal{L} = 240$ pb^{-1} collected by CDF with the two-track trigger (TTT) between March 2002 and November 2003. The data were processed using the 5.1 series of cdfsoft2 software. A sample of $D^0 \to K^-\pi^+$ decays requiring two track trigger confirmation on K^- and π^{+1} was selected from the compressed `B_CHARM`

[1] Reference to the specifuc charge state implies charge conjugate as well unless specifically noted

stream using a `BottomMods` package built with 5.3.1 version of cdfsoft2. The two track confirmation cuts imposed on K^- and π^+ candidate tracks were as follows:

- for each track the SVT match required:
  - $|\Delta\phi_{SVT-COT}| < 0.015$ rad
  - $|\Delta cu_{SVT-COT}| < 0.00015\text{cm}^{-1}$
  - $\chi^2_{SVT} < 25$
- we sort the events into paths according to the L2 trigger they passed using the Prereq module. We then require the offline track pair forming the D^0 candidate to pass the same L2 TTT requirements as was required online, and verify that they are matched to svt tracks. Appendix A lists all trigger lines allowed for this analysis. Out of idle curiosity, we then split up the total D^0 skim sample into three non-overlapping subsets defined by:
  – high pt triggers
  – standard and not high pt
  – low pt and not (standard or high pt)

The size of inclusive D^0 sample is relatively small – about 3% of the input dataset. We could keep it resident on disk and accessible via *rootd*.

An invariant mass plot of $K^-\pi^+$ combinations passing the criteria enumerated above and subjected to `CTVMFT` vertex fit with $\chi^2 < 30$ is shown in Figure 2. The superimposed curve shows a fit with a Gaussian signal function and a second order polynomial background. The signal yield is about 3M events. This number includes double counted candidates $K \leftrightarrow \pi$.

¿From that sample we ntupelized the decay chains (1) using `BStntuple` framework, a part of `BottomMods` software package, which is a simplified version of `Stntuple` tailored for particle reconstruction.

6 Candidate selection

The analysis of pentaquark states decaying to $D^{*+}\bar{p}(p)$ is similar to the analysis of D^{**} states reported recently in [7].

6.1 D^{*+} selection

The D^{*+} candidates were made by combining each D^0 candidate that had an nvariant mass within ± 20 MeV/c^2 around PDG D^0 mass with all positively charged slow pion candidate tracks having $p_T(\pi_{slow}) > 400$ MeV/c in an event. The $(D^0\pi^+_{\text{slow}})$ pairs were subjected to the vertex fit with the with the fit χ required to be less than 30. The resulting mass difference spectrum, $\mathrm{M}(\mathrm{D}^0\pi^+_{\mathrm{slow}}) - \mathrm{M}(\mathrm{D}^0)$, is shown in Figure 3 It was fit with the function:

$$\begin{aligned} \mathcal{F} = & \; N\left(\frac{1}{1+r}\cdot Gauss(x,\Delta M_1,\sigma_1) + \frac{r}{1+r}\cdot Gauss(x,\Delta M_2,\sigma_2)\right) + \\ + & \; c\cdot\left(1 - e^{\frac{x-m_\pi}{a}}\right)\left(\frac{x}{m_\pi}\right)^b \end{aligned} \tag{2}$$

where $x = \mathrm{M}(\mathrm{D}^0\pi^+_{\mathrm{slow}}) - \mathrm{M}(\mathrm{D}^0)$. The Fit results are summarized in Table 1

Signal Yield	536604 ± 860
σ_1	(0.501 ± 0.002) MeV/c^2
σ_2	(1.176 ± 0.009) MeV/c^2
r	(1.802 ± 0.037)
ΔM_1	(145.432 ± 0.001) MeV/c^2
ΔM_2	(145.652 ± 0.005) MeV/c^2

Table 1: Fit results of D^{*+}mass difference spectrum

.

6.2 D** Selection

All D^{*+} candidates having $\left|\mathrm{M}(K^-\pi^+\pi^+_{slow}) - \mathrm{M}(K^-\pi^+) - 0.1454\right| < 1.8$ MeV/c^2 were combined with π^- candidate tracks, having $p_T(\pi^+) > 500$ MeV/c and were fit to common vertex to form D**s. The vertex fit χ^2 was required to be less than 30. The resulting mass difference spectrum, $\mathrm{M}(\mathrm{D}^{*+}\pi^-) - \mathrm{M}(\mathrm{D}^{*+})$, is shown in Figure 4. The summary event yield of $\mathrm{D}_1(2420)$ and $\mathrm{D}_2^*(2460)$ was determined by subtracting the number of events in the signal region [0.37,0.5] GeV/c^{2}and the number of background events obtained from the fit to the sideband region of the 4th order polynomial multiplied by threshold factor. The number of events in D** peak is 14669 ± 323 in good agreement with the numbers reported in [6]. Having assured ourselves that we can reconstruct D** decays we proceeded to look for Θ_c.

6.3 $\mathrm{D}^{*+}\bar{\mathrm{p}}$ selection

The selection of $(\mathrm{D}^{*+}\bar{\mathrm{p}})$ candidates is identical to the selection of $(\mathrm{D}^{*+}\pi)$ discussed in the previous subsection, except that the proton mass is used for the fourth track. No particle ID is applied at the selection stage. The mass difference plot of $(\mathrm{D}^{*+}\bar{\mathrm{p}}$ combinations is shown in Figure 5, the quantity plotted is mass difference plus the nominal D^{*+} mass. Clearly there is no visible signal at the mass of 3.099 MeV/c^2.

We performed an unbinned maximum likelihood fit To extract an upper limit on the event yield at the 3.099 MeV/c^2 mass, we preformed an unbinned maximum likelihood fit using the following log likelihood function:

$$\begin{aligned} F = -2\ln\mathcal{L} &= \mathcal{F}(\vec{\alpha}) - \sum_{i}^{N} \ln f(x_i, \vec{\alpha}) + \\ &+ GC(m) + GC(\sigma) \end{aligned}$$

where $\mathcal{F}(\vec{\alpha}) = \int_a^b f(x, \vec{\alpha})dx$, a and b are integration limits (0.9 GeV/c^{2}and 1.4 GeV/c^2) and

$$\begin{aligned} f(x_i, \vec{\alpha}) &= G \otimes BW(x_i, \sigma, \Gamma, M) + \\ &+ \sqrt{(x_i - M_p)} \cdot \sum_{j=0}^{3} (x_i - (M_p))^j \end{aligned}$$

and $GC(\sigma)$ and $GC(m)$ are Gaussian constraints on σ (2.5 ± 0.2 MeV/c^2) and mass of the pentaquark, the latter was determined by H1 to be $3,099 \pm 6$ MeV/c^2. The former is the detector resolution for the mass difference plotted, as determined using realistic Monte Carlo simulation. At this point the natural width of pentaquark was fixed to zero. Figure 5 show the superimposed result of the fit. The fit quality was found to be $\chi^2/ndf = 1.1$. Figure 7 show the likelihood profile as the function of the number of events, the upper limits corresponding to 90% and 95% confedence level intervals are marked red and blue correspondingly. We determined the upper limit on the event yields to be 29 90% CL (37 95 % CL).

7 Proton Selection

Particle identification for the proton tracks is a crucial piece of the analysis. Because the predicted range of proton momenta starts near 1 GeV/c and goes above 8 GeV/c, according to simulation, we must use both time of flight (TOF) and dE/dx techniques. The dE/dx validation follows the B group studies led by the Italian B group in CDF note 6932 [8].

7.1 Proton TOF study

We have ntupelized decays $\Lambda \to p\pi$ from compressed inclusive hadronic dataset xbhd0c. A fraction of the total sample was used in this analysis to verify ToF and dE/dx. The Λ hyperons were reconstructed from opposite charge pairs of tracks satisfying the following criteria:

- `numCTHitsAx`> 19, `numCTHitsSt`> 15 on both legs
- $p_T(\mathrm{p}) > \mathrm{p_T}(\pi)$
- $|\Delta z| < 5$ cm at tracks intersection point

- $\cos(\alpha) > 0.998$, where α is the angle between Λ candidate momentum vector and the vector connecting primary and Λ vertices.
- `CTVMFT` fit
- $L_{xy} > 1$ cm
- $\chi^2 < 49$
- $|d_0(p)| > 0.05$ cm
- $|d_0(\pi)| > 0.05$ cm
- no SVT-match requirement on proton
- $\left| m(\pi^+\pi^-) - M_{K^0_S} \right| > 20$ MeV/c^2 after proton$\rightarrow \pi$ mass re-assignment

The resulting invariant mass spectrum is shown in Figure 8. The superimposed curve shows the result of the fit to two Gaussians to represent a signal and polynomial background multiplied by square root threshold factor. The event yielded 1.3 million Λ decays. Gaussian resolutions were found to be $\sigma_1 = (1.182 \pm 0.005)$ MeV/c^2 and $\sigma_2 = (3.470 \pm 0.005)$ MeV/c^2.

We proceeded to study TOF pull distributions for protons defined as:

$$Pull(TOF)_{p,\pi} = \frac{TOF(mes) - TOF(exp)_{p,\pi}}{\sigma_{TOF}}$$

Both, the measured TOF(mes) and expected $TOF(exp)_{p,\pi}$ were corrected for Λ lifetime. The latest TOF software from 5.3.1int1 was used. The $TOF(exp)_{p,\pi}$ is expected TOF for a given particle hypothesis. We checked proton and pion hypotheses to study p/π separation. We fit sideband subtracted TOF pull distributions in bins of proton transverse momentum with Gaussians to obtain pulls' mean values. The Λ signal region was defined as

$$|m(p\pi) - M_\Lambda| < 3 \cdot 0.003,$$

the sideband region was defined as

$$4 \cdot 0.003 < |m(p\pi) - M_\Lambda| < 7 \cdot 0.003.$$

Note that usage of TOF information comes at the price of halving the data sample due to about 50% TOF efficiency.

The example TOF pull plots for four proton transverse momentum bins are shown in Figure 9. Red shows pulls for proton mass hypothesis. Blue shows pion mass hypothesis. The summary TOF separation plot is presented in Figure 10. It can be seen that p/π separation of 2σ can be maintained up to 2.75 GeV/c of proton transverse momentum. We will apply 2σ cut on proton pull for $p_T < 2.75$ GeV/c for pentaquark analysis with TOF. The estimated efficiency of 2σ TOF cut for protons is presented in Figure 11. If the TOF pulls were ideally Gaussian the efficiency of such a cut would have been 95%. The measured values are slightly below 90% indicating the presence of non-Gaussian tails in pull distributions. This warrants further study of TOF performance

7.2 $D^{*+}\bar{p}$ with TOF cut

An invariant mass spectrum of $D^{*+}\bar{p}$ combinations after applying 2σ TOF PId cut is shown in Figure 12. The fit quality is $\chi^2/ndf = 1.3$ The upper limits on the numbers of events are 12 (90% CL) and 15 (95% CL).

7.3 dE/dx PID studies with Λs and D^{*+} samples

We tried to apply the universal curve obtained in [8] to study proton pulls and discovered that this curve does not describe well the low β region. We thus determined the universal curve ourselves using :

- SVT triggered K and π from D^0 decays requiring D^0 to be originated from D^{*+} for purity
- protons from Λ decays in TTT data. No requirement on SVT-proton match was used.

We used dE/dx corrections according to Ref. [8]. The dE/dx for negative pions was shifted upwards by 0.18 ns, as specified in [8]. Figures 14 and 15 show mean dE/dx as a function of the track's Lorenz boost $\beta\gamma$. The mean dE/dx in each $\beta\gamma$ bin were obtained using sideband subtracted samples of protons, pions, and kaons from Λ and D^*'s. We then fitted the resulting dE/dx distributions to a single Gaussian. The fit to the "standard CDF universal curve" expressed as

$$\frac{dE}{dx} = \frac{1}{\beta^2}\left(c_1 \cdot \log\left(\frac{\beta\gamma}{\beta\gamma + b}\right) + c_0\right) + a_1(\beta - 1) + a_2(\beta - 1)^2.$$

produced the following parameter set:

parameter	positive track	negative track
c_0	20.37 ± 0.06	22.34 ± 0.13
c_1	2.32 ± 0.02	2.33 ± 0.02
b	105.62 ± 5.02	248.26 ± 18.92
a_1	-23.77 ± 0.29	-24.09 ± 0.29
a_2	-30.26 ± 0.73	-32.44 ± 0.82

Having obtained the universal curve we can then calculate the expected dE/dx for a given mass hypothesis. Again, similar to the TOF study we defined a dE/dx pull as:

$$Pull(dE/dx)_{p,\pi} = \frac{dE/dx(mes) - dE/dx(exp)_{p,\pi}}{\sigma_{dE/dx}}$$

The examples, of sideband subtracted pulls for proton (red) and pion hypothesis (blue) are shown in Figure 16 shows dE/dx pulls for the sideband subtracted proton samples. Depicted are proton (red) and pion (blue) hypothesis for the proton sample for for different momentum bins.

The summary dE/dx separation plot is presented in Figure 17. A pair of red and blue points for a given momentum bin is obtained by plotting the dE/dx pulls for the proton sample for proton and pion hypothesis, and recording the mean of these pulls.

Figure 17 indicates a p/π separation of $\sim 1.3\sigma$ starting from 2.75 GeV/c of proton transverse momentum. We thus required —dE/dx pull—< 1.3 for protons of $p_T > 2.75$ GeV/c for the part of the pentaquark analysis that uses dE/dx.

7.4 $\mathrm{D}^{*+}\bar{\mathrm{p}}$ with dE/dx cut

An invariant mass spectrum of $\mathrm{D}^{*+}\bar{\mathrm{p}}$ combinations after applying the aforementioned dE/dx PId cut is shown in Figure 18. The fit quality is $\chi^2/ndf = 1.2$. The upper limits on the numbers of events are 19 (90% CL) and 24 (95% CL).

8 Conclusion

Using a high statistics D^{*+} sample collected with the displaced track trigger we searched for a narrow exotic baryon decaying to $\mathrm{D}^{*+}\bar{\mathrm{p}}$. No excess yield above background was found and the upper limit on the event yield was obtained to be 29 and 37 events 90% and 95% CL respectively. We utilized particle identification capabilities of the CDF detector and applied separately TOF and dE/dx particle id cuts for proton candidate tracks below and above 2.75 GeV/c. No evidence for exotic baryons was found.

A L2 Trigger criteria

One of the following L2 trigger criteria was required for events to be included in this analysis.

```
Standard triggers

      Level 2 Trigger Bit                         Specific Option
      -------------------                         ---------------

L2_TWO_TRK2_D100_PS10_L1_SEVEN_TRK2_v-1          L2_TWO_TRK2_D100_v-1
L2_TWO_TRK2_D100_L1_OPPQ_DPHI135_SUMPT5.5_v-1    L2_TWO_TRK2_D100_v-2
L2_TWO_TRK2_D100_PS10_L1_SEVEN_TRK2_v-2          L2_TWO_TRK2_D100_v-2
L2_TWO_TRK2_D100_L1_SEVEN_TRK2_v-3               L2_TWO_TRK2_D100_v-2
L2_B_CHARM_v-1                                   L2_B_CHARM_v-1
L2_B_CHARM_L1_DPS_v-1                            L2_B_CHARM_v-1
L2_B_CHARM_L1_SEVEN_TRK2_v-1                     L2_B_CHARM_v-1
L2_B_CHARM_L1_DPS_v-2                            L2_B_CHARM_v-2
L2_B_CHARM_L1_SEVEN_TRK2_v-2                     L2_B_CHARM_v-2

Low Pt triggers

      Level 2 Trigger Bit                         Specific Option
      -------------------                         ---------------
```

```
L2_B_CHARM_LOWPT_v-1                          L2_B_CHARM_LOWPT_v-1
L2_B_CHARM_LOWPT_L1_SEVEN_TRK2_v-1            L2_B_CHARM_LOWPT_v-1
L2_B_CHARM_LOWPT_L1_DPS_v-1                   L2_B_CHARM_LOWPT_v-1
L2_B_CHARM_LOWPT_L1_DPS_v-2                   L2_B_CHARM_LOWPT_v-2

High Pt triggers

      Level 2 Trigger Bit                       Specific Option
      -------------------                       ---------------

L2_B_CHARM_HIGHPT_v-1                         L2_B_CHARM_HIGHPT_v-1
L2_B_CHARM_HIGHPT_L1_SEVEN_TRK2_v-1           L2_B_CHARM_HIGHPT_v-1
L2_B_CHARM_HIGHPT_v-2                         L2_B_CHARM_HIGHPT_v-2
L2_B_CHARM_HIGHPT_L1_SEVEN_TRK2_v-2           L2_B_CHARM_HIGHPT_v-2
L2_B_CHARM_HIGHPT_v-3                         L2_B_CHARM_HIGHPT_v-3
L2_B_CHARM_HIGHPT_L1_SEVEN_TRK2_v-3           L2_B_CHARM_HIGHPT_v-3
```

References

[1] Diakonov, Petrov, and Polyakov, Z. Physik A **359**, 308 (1997).

[2] Jaffe, R. and F. Wilczek, Phys. Rev. Lett. **91**, 232003 (2003), hep-ex/0307341.

[3] Aktas, A. *et al.*, hep-ex/0403017.

[4] T. Yamashita *et al.*, "Measurement of the Run-II Inclusive J/Psi Cross-section" CDF/PHYS/BOTTOM/CDFR/6288

raggedright

[5] Particle Data Group, K. Hagiwara *et al.*, Phys. Rev. **D 66**, 2002

[6] M. Campanelli, E. Gerchtein "Calibration of the momentum scale for Kalman refitter using J/ψ events" CDF/PHYS/BOTTOM//6905

[7] M. Campanelli, E. Gerchtein "Measurement of mass and width of the orbitally- excited charmed mesons D_1 (2420) and D_2 (2460)" CDF/PHYS/BOTTOM/CDFR/6918

[8] S. D'Auria *et al.*, "Track-based calibration of the COT specific ionization", CDF/ANAL/BOTTOM/CDFR/6932

[9] F. Curbis *et al.*, "Search for the pentaquark $\Theta+ \to pK^0_S$ in CDF Run II data" CDF/PHYS/BOTTOM/CDFR/6975

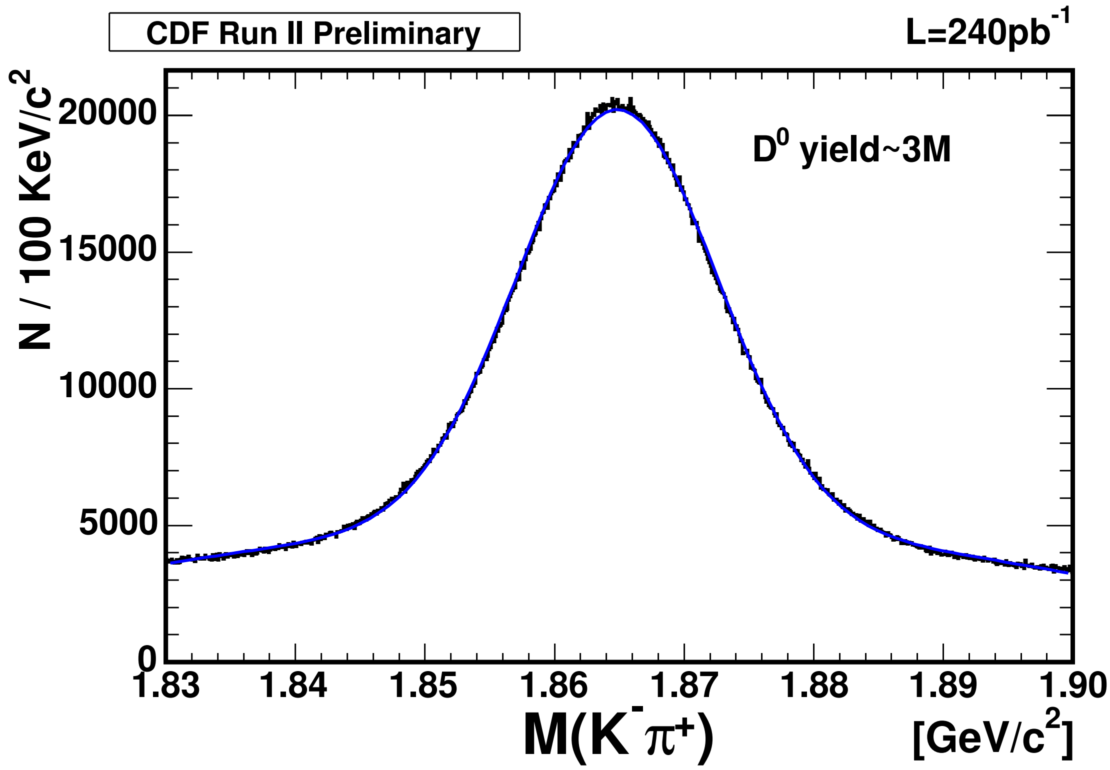

Figure 2: An invariant mass of $K^-\pi^+$ combination. The smooth curve represents fit described in the text

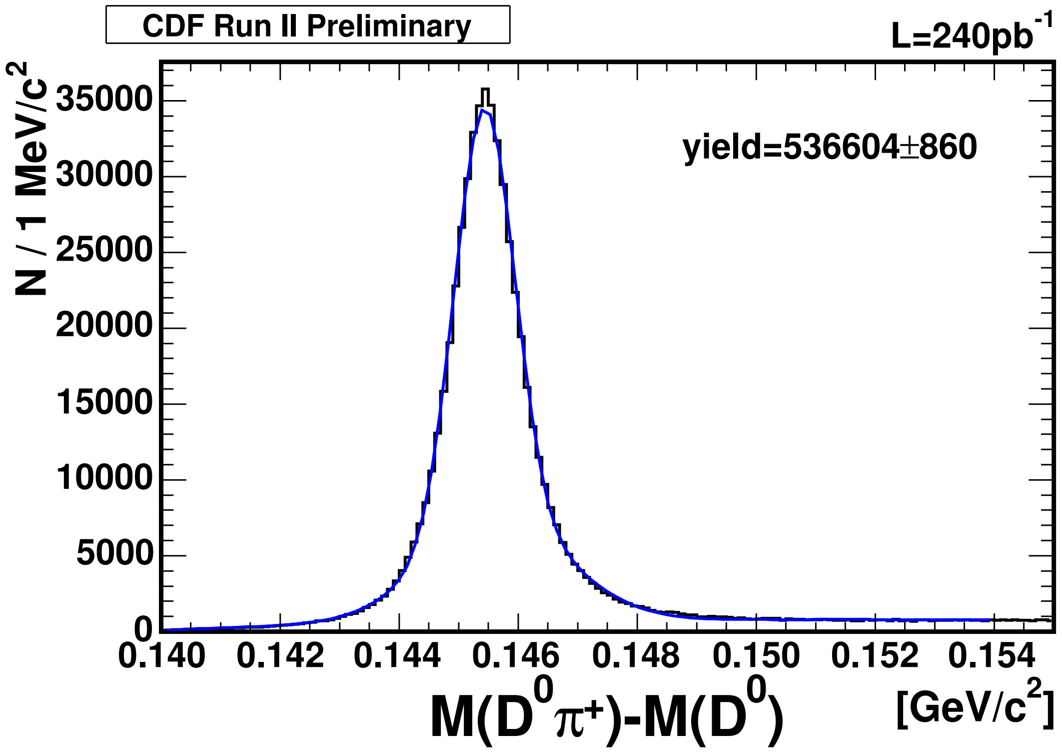

Figure 3: A D^{*+} mass difference spectrum. Superimposed curve shows the result of the fit described in the text.

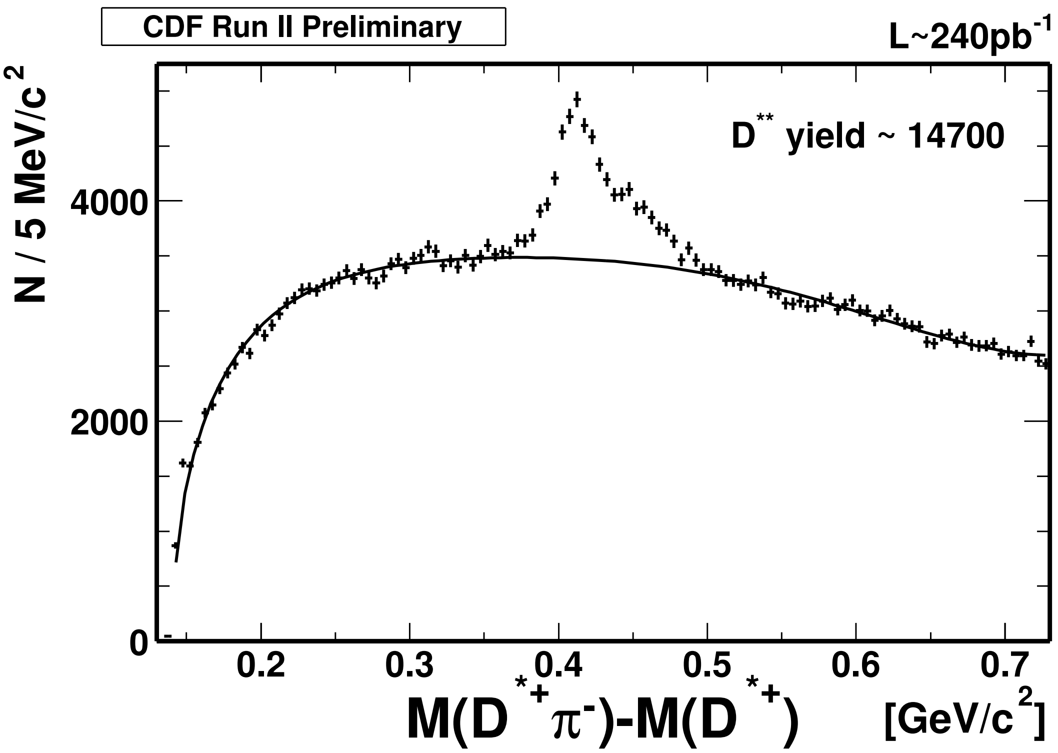

Figure 4: A D** mass difference spectrum

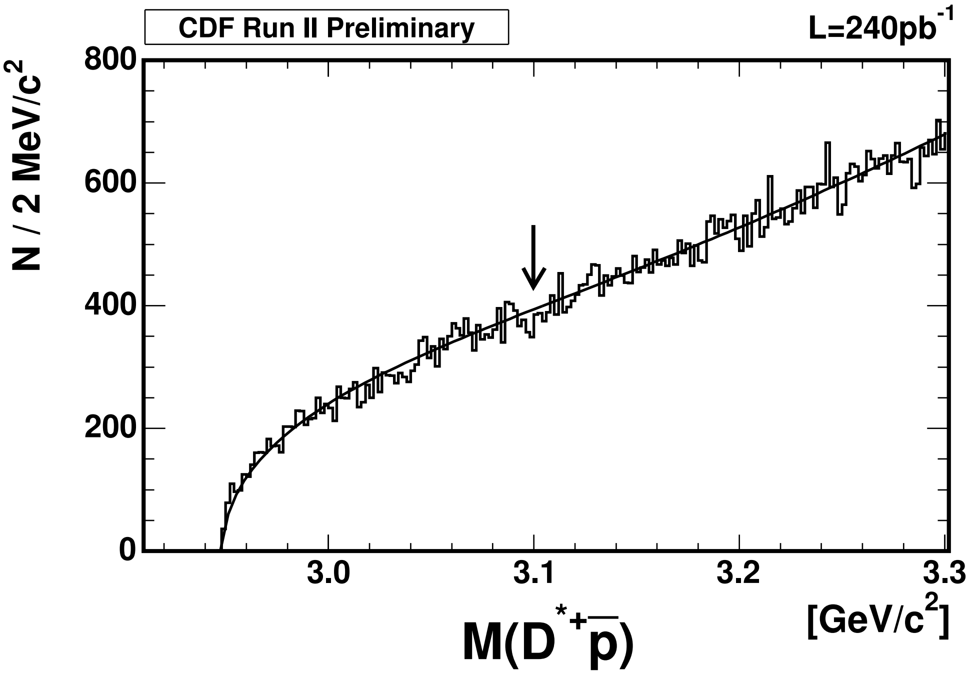

Figure 5: A ($D^{*+}\bar{p}$) mass difference spectrum ($\Delta M + M_{D^*}$) without proton PID. The smooth curve represents the fit described in the text

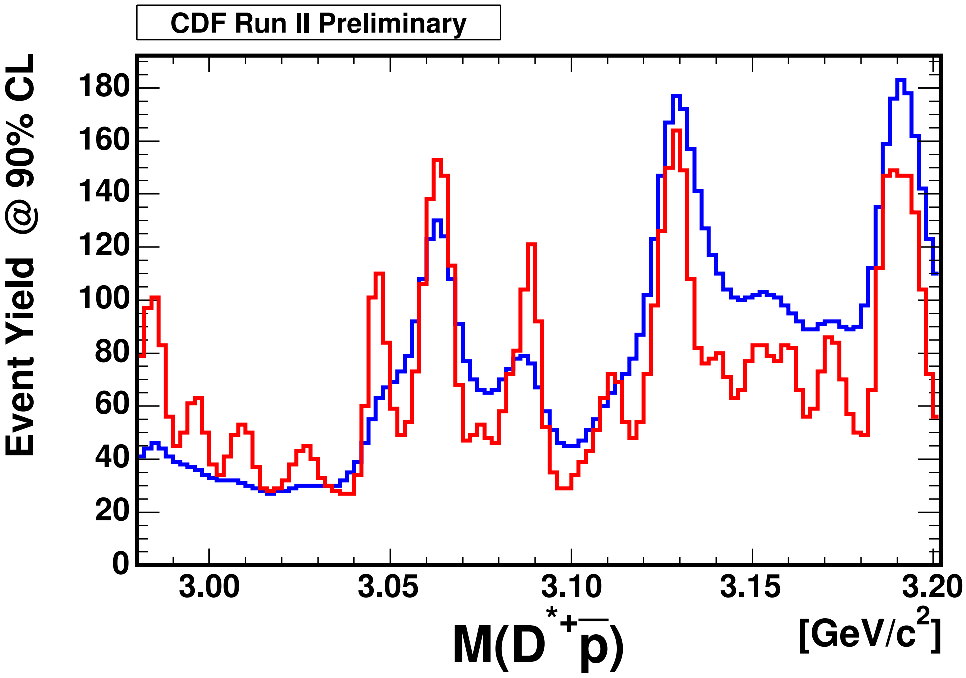

Figure 6: Event yield at 90% CL level as the function of mass. Red curve shows represent zero natural width, blue curve shows results for $\Gamma = 12$ MeV/c^2

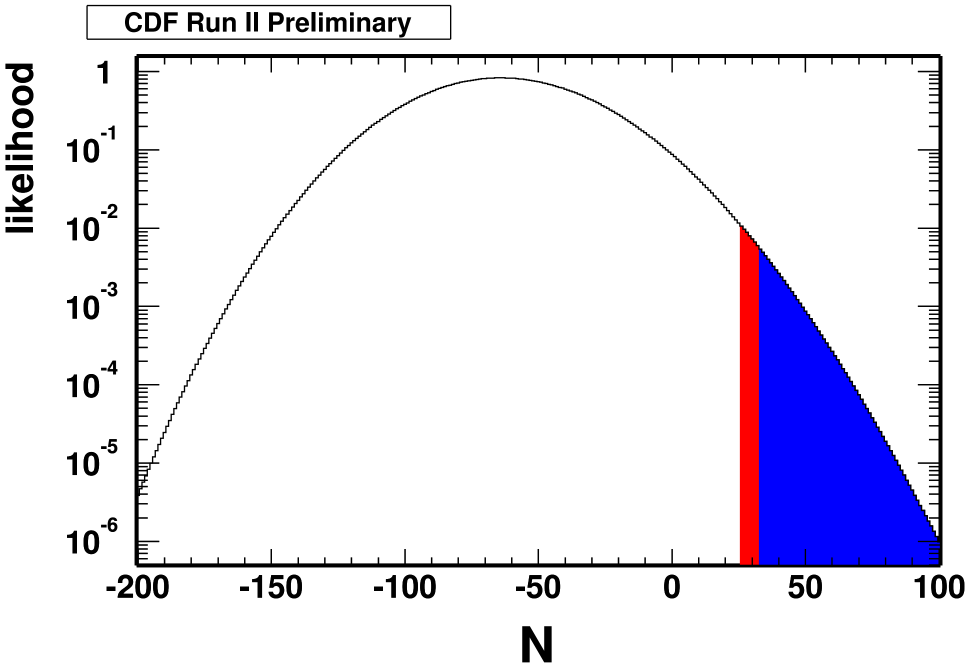

Figure 7: A likelihood profile vs number of events. Red band marks 90% confidence level, blue band marks 95% confidence level.

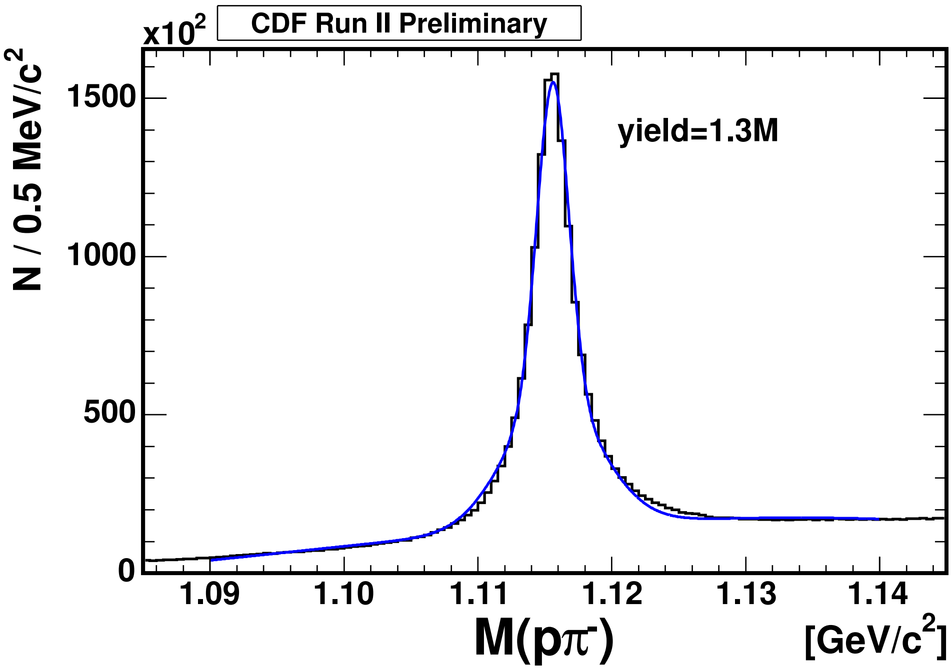

Figure 8: An invariant mass of pπ^- combination.

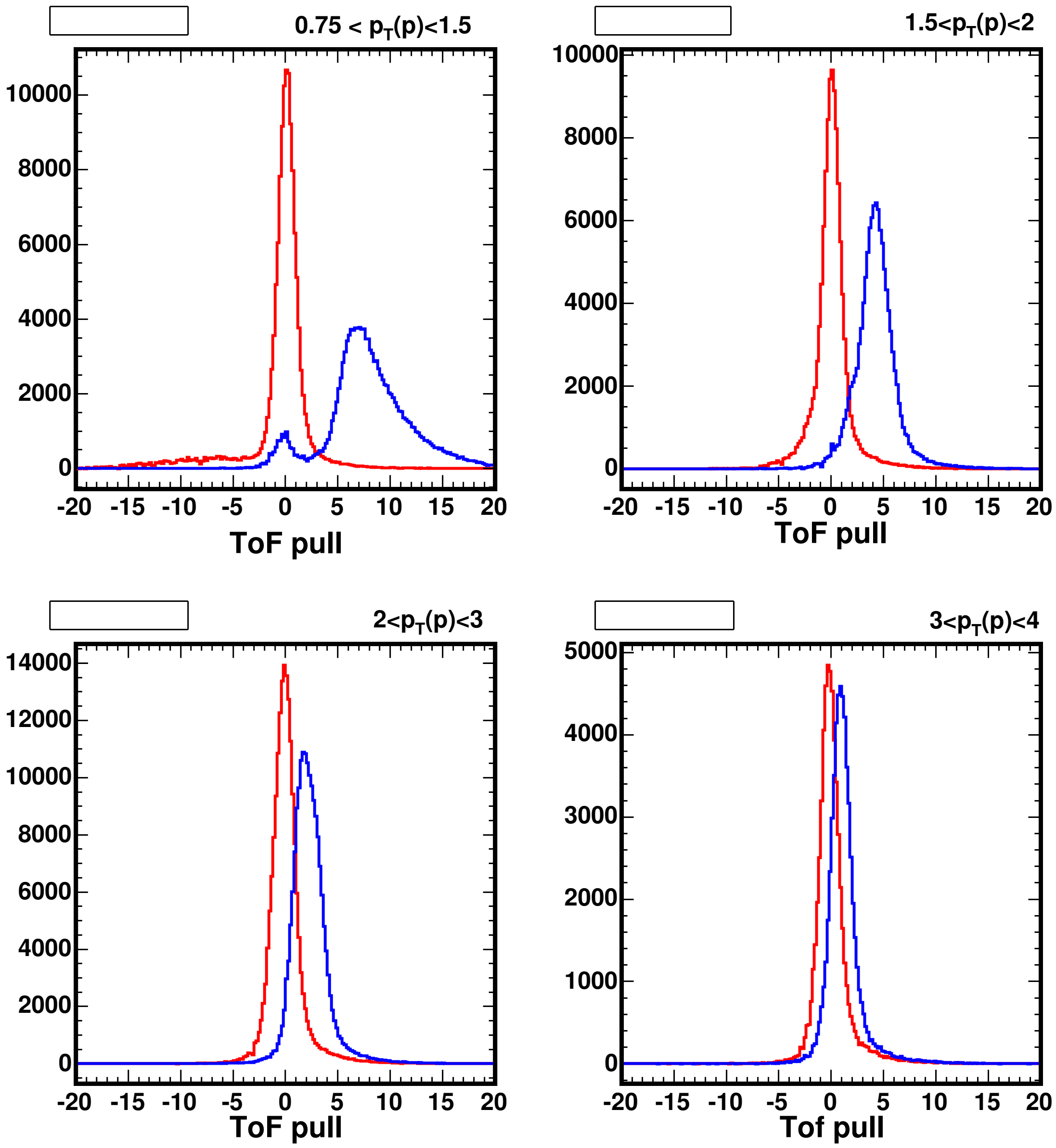

Figure 9: TOF pulls for protons in different p_T bins. Red shows pulls for proton mass hypothesis. Blue shows pion mass hypothesis.

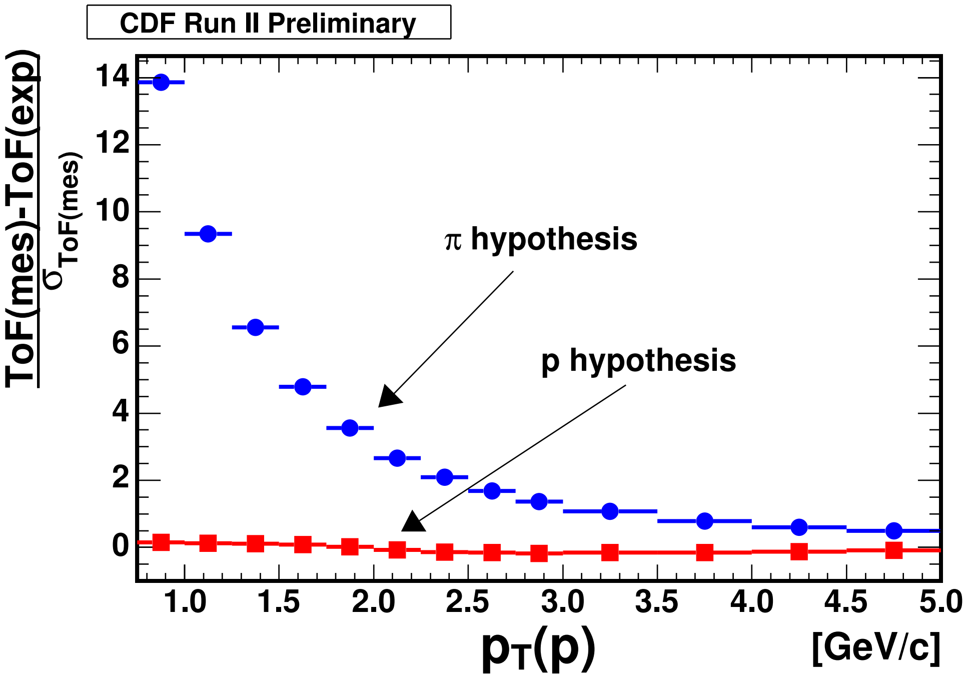

Figure 10: p/π separation based on TOF information expressed in the units of TOF sigma

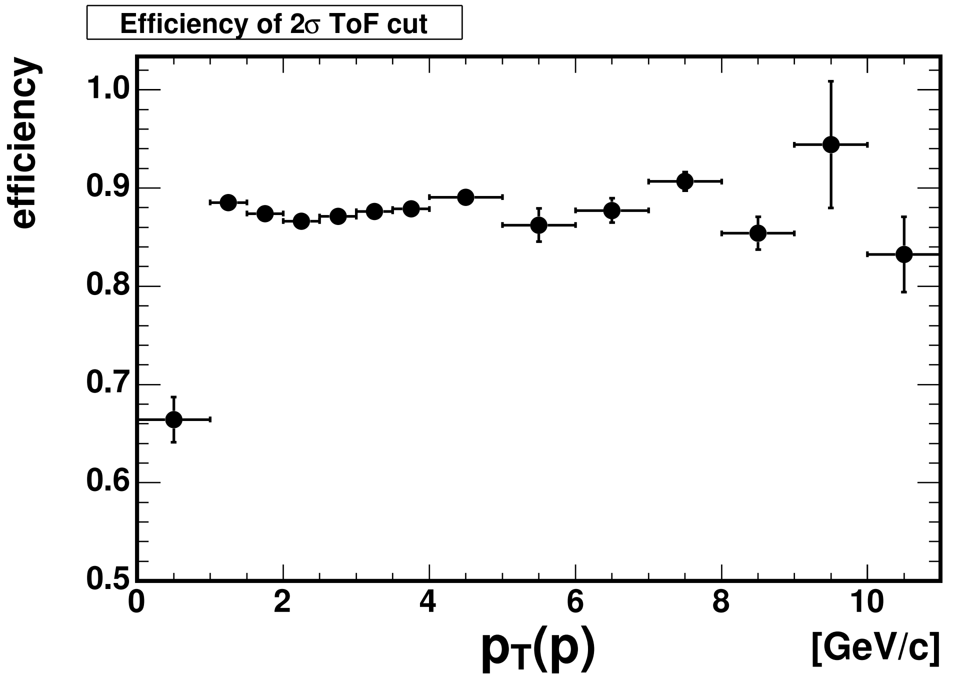

Figure 11: The efficiency of 2σ TOF cut as the function of proton transverse momentum

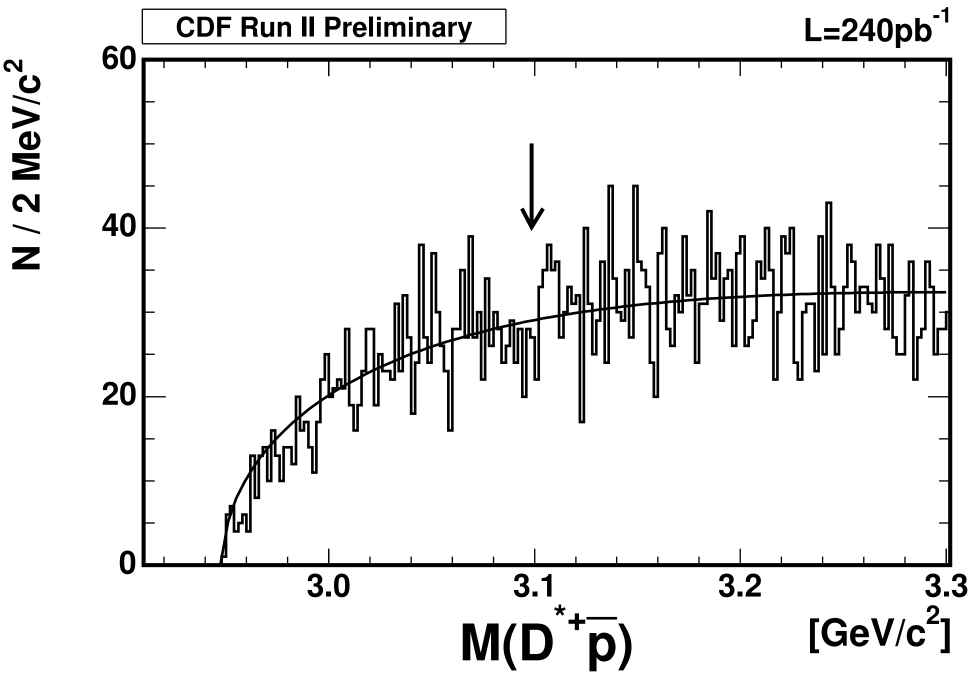

Figure 12: The $D^{*+}\bar{p}$ mass spectrum after applying 2σ TOF cut

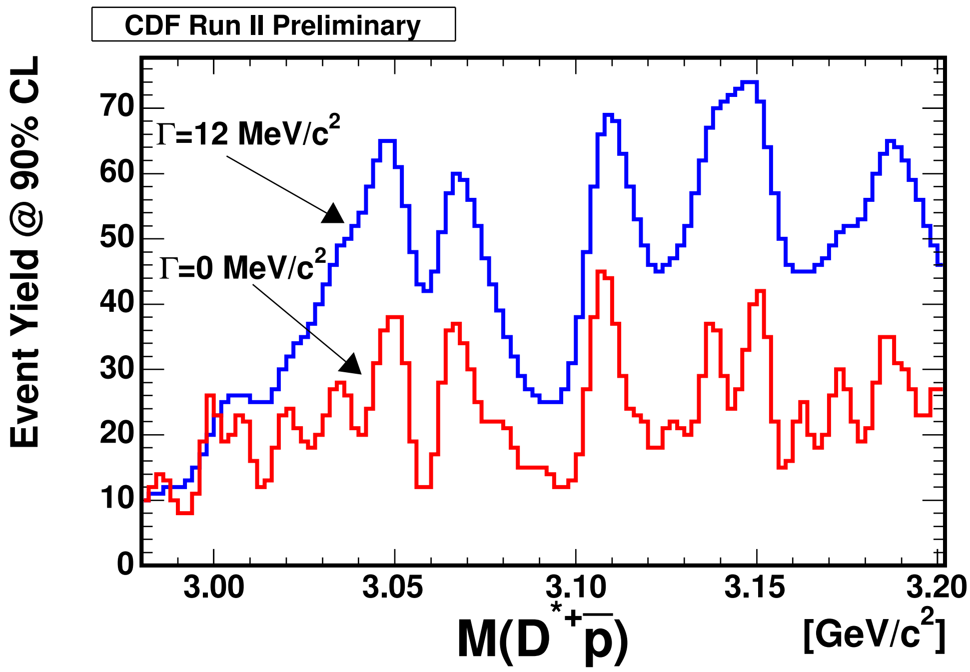

Figure 13: Event yield at 90% CL level as the function of mass. Red curve shows represent zero natural width, blue curve shows results for $\Gamma = 12$ MeV/c^2

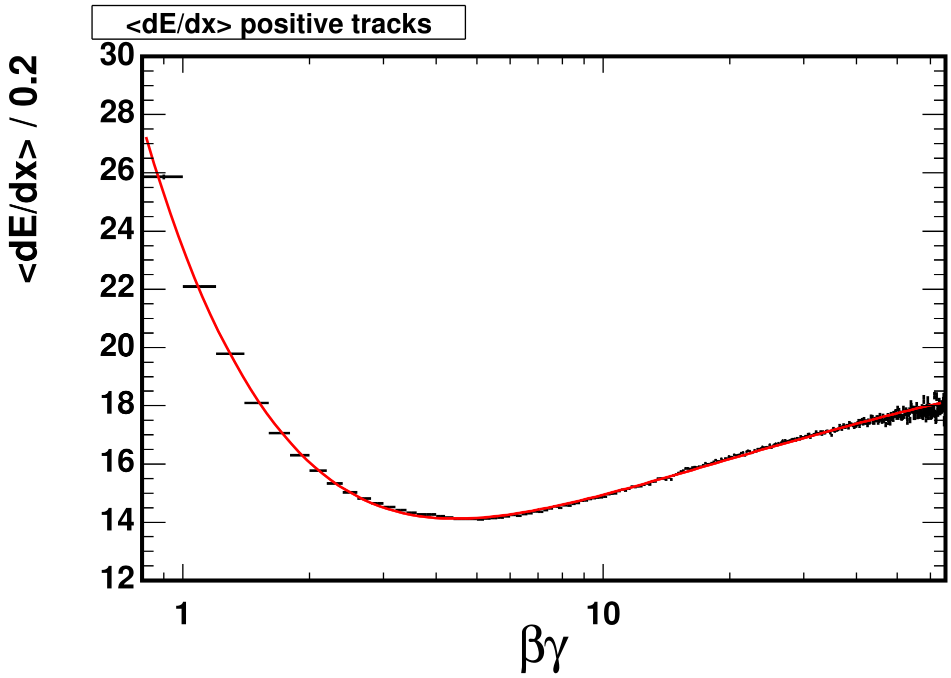

Figure 14: Mean positive track's dE/dx vs $\beta\gamma$

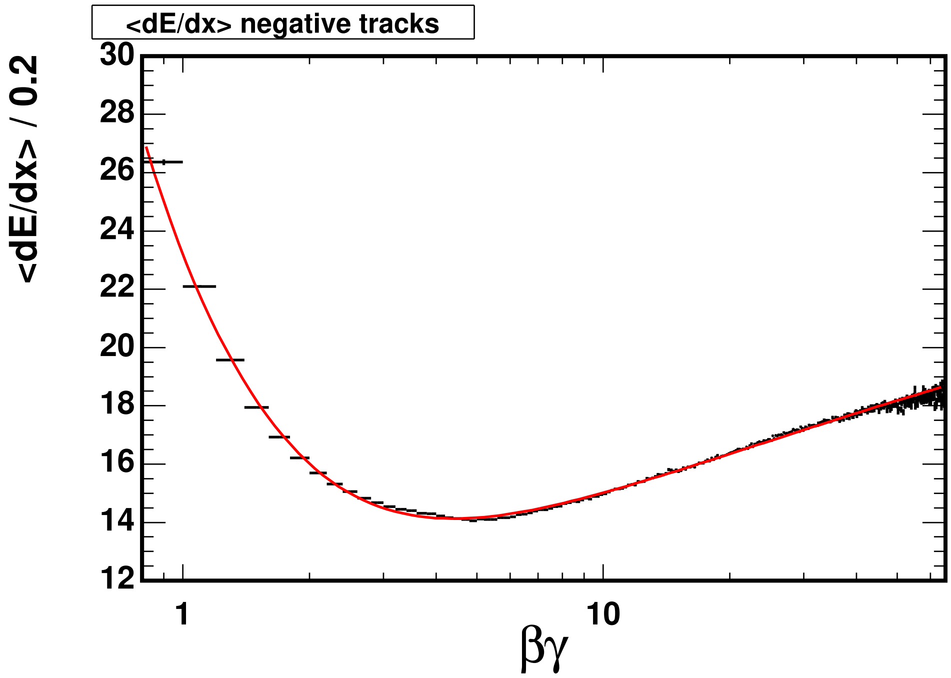

Figure 15: Mean negative track's dE/dx vs $\beta\gamma$

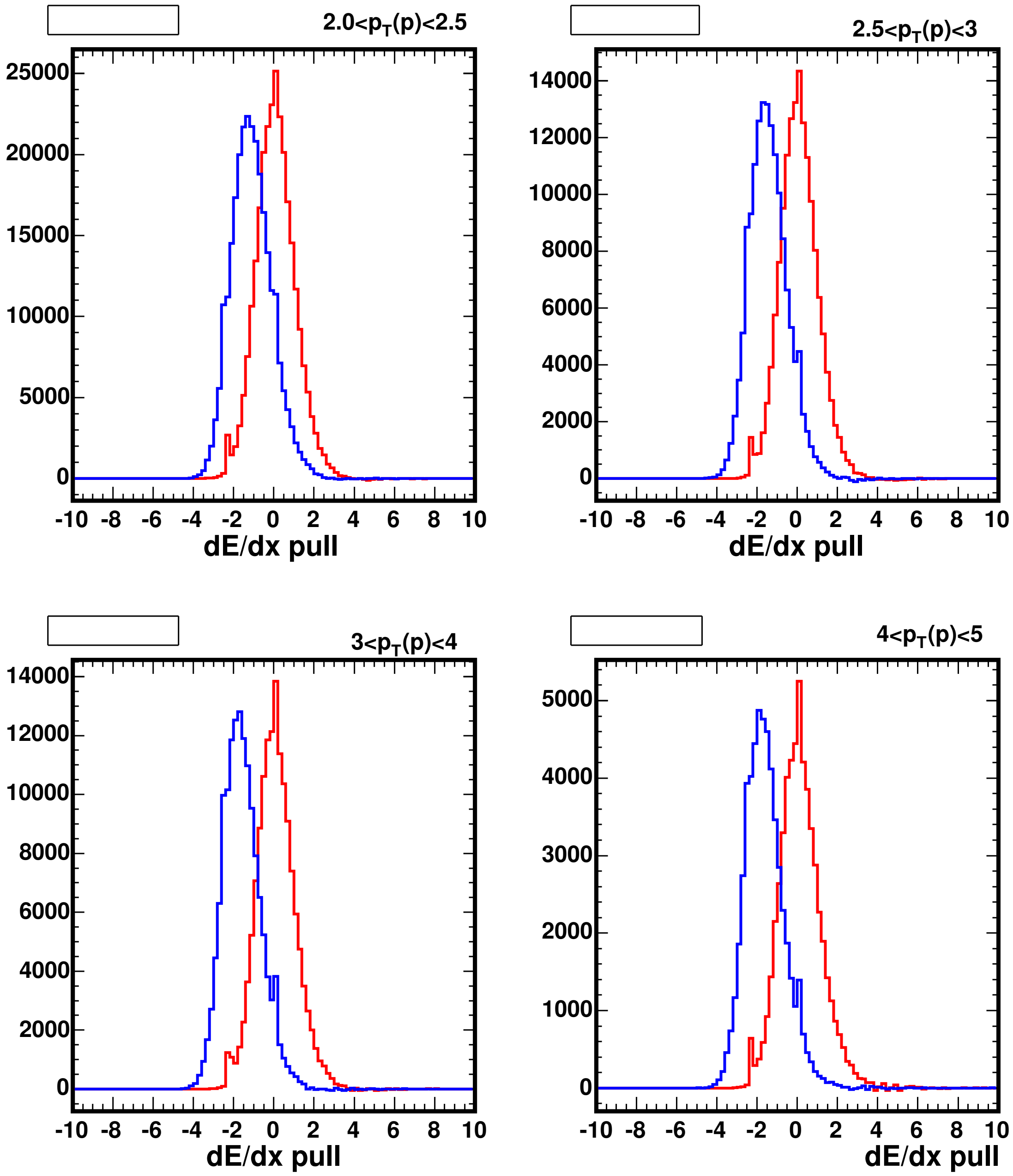

Figure 16: dE/dx pulls for protons in different p_T bins. Red shows pulls for proton mass hypothesis. Blue shows pion mass hypothesis.

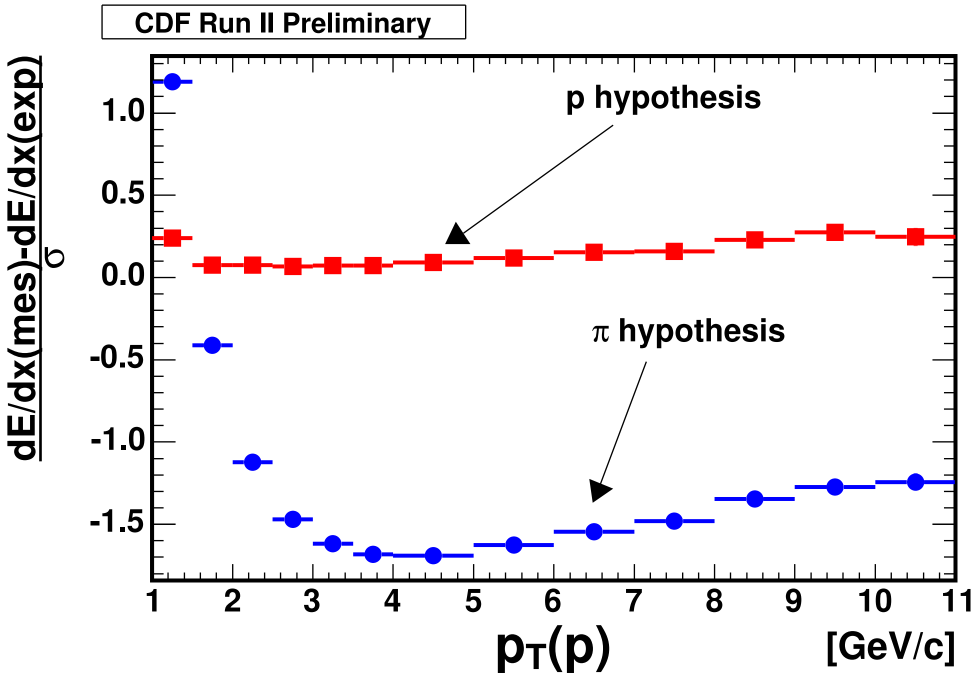

Figure 17: p/π separation based on dE/dx information expressed in the units of dE/dx sigma

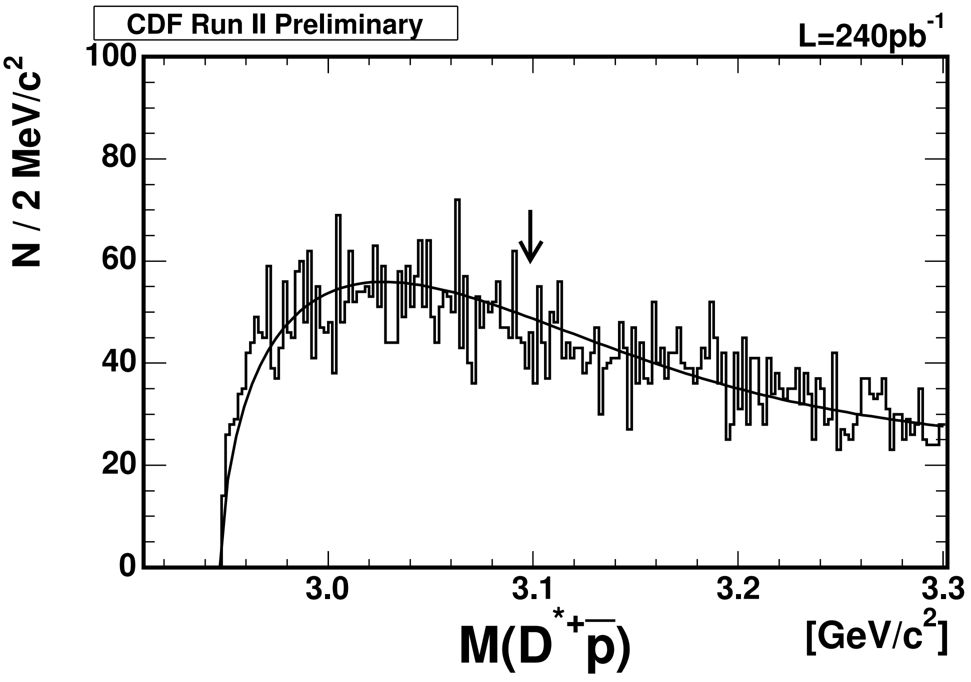

Figure 18: An invariant mass spectrum of $D^{*+}\bar{p}$ combinations after applying cut $Pull(dE/dx)_p < 1.3$ and $p_T(p) > 2.75$ GeV/c.

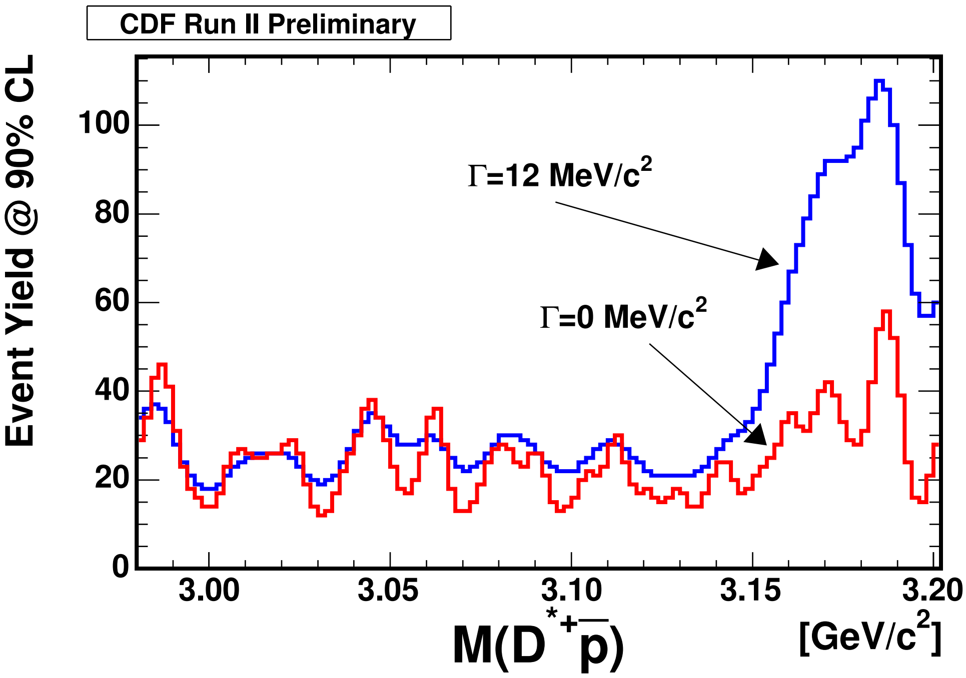

Figure 19: Event yield at 90% CL level as the function of mass. Red curve shows represent zero natural width, blue curve shows results for $\Gamma = 12$ MeV/c^2